AIAA-2003-1716
A Model to Compare the Flight Control Energy Requirements of Morphing and Conventionally Actuated Wings

C. O. Johnston, D. A. Neal, L. D. Wiggins.
H.H. Robertshaw, W.H. Mason and D.J. Inman
Virginia Polytechnic Institute and State University
Blacksburg, VA

11th AIAA/ASME/AHS
Adaptive Structures Conference
7-10 April 2003 / Norfolk, VA

A MODEL TO COMPARE THE FLIGHT CONTROL ENERGY REQUIREMENTS OF MORPHING AND CONVENTIONALLY ACTUATED WINGS

Christopher O. Johnston[*], David A. Neal[†], Leonard D. Wiggins[†], Harry H. Robertshaw[‡], William H. Mason[§], and Daniel J. Inman[¶]

Center for Intelligent Material Systems and Structures
Department of Mechanical Engineering
Virginia Polytechnic Institute and State University
Blacksburg, Virginia 24061

Abstract

This work presents a theoretical analysis of the actuation energy requirements of a morphing aircraft. Morphing aircraft lack discrete control surfaces and use distributed actuation of the wing surface for maneuvering. An adaptive camberline is designed that generates morphed wing shapes in response to variations in leading and trailing-edge camber. Aerodynamic energy expressions are derived from the camberline functions using a unique energy computation stemming from the vortex lattice method (VLM). Beam theory is applied to morphing airfoil sections situated along the wingspan to obtain closed-form strain energy expressions. The resulting work expressions are combined and energy optimal wing deflections are found using Lagrange multipliers. In the optimization, total energy is the cost function and constraints are placed on achieving commanded changes in lift and moment coefficients. The functions are numerically implemented to compare work expressions for a wing with morphing inputs and a conventional wing, with inboard and outboard flaps. It is shown analytically that morphing aircraft have the capability to outperform conventional vehicles in terms of required flight control energy. This work also provides a theoretically sound methodology for morphing wing energy analysis that can be applied in future trade studies of morphing vehicles.

Introduction

Morphing aircraft are a topic of current research interest[1] in the aerospace community. Such aircraft allow shape optimization over the entire flight regime[2,3] in addition to enhanced combat performance by allowing arbitrary vehicle orientation while tracking challenging flight paths. Of recent interest is the possibility of producing minimum energy control deflections by using the distributed actuation capability of morphing vehicles.

Petit's[4] work demonstrated an initial morphing wing analysis based on conformal mapping. His analysis included a numerical computation of the aerodynamic energy response in tracking a flight path. This work builds upon that analysis but approaches the problem in a different manner. As opposed to conformal mapping, the analysis begins at the camberline in terms of a load distribution and derives full analytical expressions for the aerodynamic energy requirements while morphing.

Gern[5] used *NASTRAN* to determine the energy requirements of a morphing and conventional wing in rolling maneuvers. As opposed to a numerical calculation of the energy requirements, this work presents a closed-form expression for the aerodynamic and strain energy functions allowing theoretical insight to be gained into the optimization.

Other works[4,5,6] have investigated the energy relations of morphing wings but have not presented a general method that is comprehensive enough to proceed with an in-depth analysis. The design of an adaptive camberline function facilitates the use of the VLM energy method and beam theory to derive general energy relations for the vehicle and perform a direct comparison with a conventional aircraft.

The next section covers the analytical design of the morphing camberline, followed by the derivation of the closed-form strain energy expressions, and the aerodynamic energy development. We then illustrate the optimization technique via a simple example problem. The paper concludes with numerical work comparisons of a morphing and conventional wing.

Adaptive Camberline Derivation

The first requirement for morphing analysis is the design of a camberline that will generate morphed wing shapes in response to control inputs. A morphed wing shape is defined by a wing that exhibits changes in

[*] Graduate Student, Department of Aerospace and Ocean Engineering, Student Member AIAA
[†] Graduate Student, Department of Mechanical Engineering
[‡] Professor, Department of Mechanical Engineering
[§] Professor, Department of Aerospace and Ocean Engineering, Associate Fellow AIAA
[¶] George R. Goodson Professor, Department of Mechanical Engineering

leading and trailing-edge camber. The standard camberline equations for a NACA 4-series airfoil are[7]

$$\frac{\eta}{c} = \varepsilon(x/c)^2 + \kappa(x/c) + \sigma \qquad \left(\frac{x}{c}\right) < P$$
$$\frac{\eta}{c} = \beta(x/c)^2 + \chi(x/c) + \mu \qquad \left(\frac{x}{c}\right) \geq P \tag{1}$$

where

$$\varepsilon = -\frac{M}{P^2} \qquad \kappa = \frac{2M}{P} \qquad \sigma = 0$$
$$\beta = -\frac{M}{(1-P)^2} \quad \chi = \frac{2MP}{(1-P)^2} \quad \mu = \frac{M(1-2P)}{(1-P)^2} \tag{2}$$

In equations (1) and (2), c is the chord length while M and P are the nondimensional magnitude and location of maximum camber, respectively.

To adapt the camberline functions for morphing we attach an additional shape function at some location along the chordline, such that the magnitude and slope at the connection are equal. The slope at the trailing edge is then defined by a separate control input as illustrated in Figure 1.

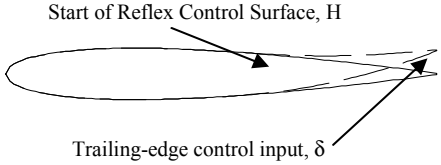

Figure 1. Trailing-edge wing control

With the addition of a trailing-edge camberline function, the equations in (1) become

$$\frac{\eta}{c} = \varepsilon(x/c)^2 + \kappa(x/c) + \sigma \qquad \left(\frac{x}{c}\right) < P$$
$$\frac{\eta}{c} = \beta(x/c)^2 + \chi(x/c) + \mu \quad H > \left(\frac{x}{c}\right) \geq P \tag{3}$$
$$\frac{\eta}{c} = \phi(x/c)^2 + \upsilon(x/c) + \xi \qquad \left(\frac{x}{c}\right) \geq H$$

where H locates the start of the trailing edge control surface. The initial coefficients (ε, κ, σ, β, χ, μ) stay the same while the new trailing-edge coefficients are defined as

$$\phi = \frac{M(P-H)}{(H-1)(1-P)^2} - \frac{0.5\delta}{(H-1)}$$
$$\upsilon = \frac{-2M(P-H)}{(H-1)(1-P)^2} + \frac{H\delta}{(H-1)} \tag{4}$$
$$\xi = \frac{M\left(1-2P+2PH-H^2\right)}{(1-P)^2} - \frac{MH(H-2)(P-H)}{(1-P)^2(H-1)} - \frac{0.5\delta H^2}{(H-1)}$$

where δ is the trailing-edge control angle measured relative to the horizontal axis.

For a fixed control surface size and maximum camber location, equations (3) and (4) define a morphed wing shape in response to control inputs of maximum camber and desired trailing-edge deflection angle. The adaptive camberline equation allows an airfoil to achieve both a commanded ΔC_L and ΔC_M irrespective of angle of attack. The structure of these expressions is convenient for the application of traditional aerodynamic and beam theory for morphing wing analysis.

Morphing Strain Energy

To perform a complete energy analysis, it is necessary to have an analytical strain energy function that correlates to morphing deflections. Using the camberline functions from equations (3) and (4), an inverse approach to beam theory solutions can be used to determine the required strain energy to create adaptive wing shapes.

From elementary calculus and mechanics of deformable bodies[8] the beam shape resulting from a distributed moment is

$$\frac{d^2y}{dx^2} = \frac{M(x)}{EI(x)} \tag{5}$$

In beam analysis equation (5) is generally solved for the resulting beam deflections. As opposed to a beam, equation (5) can be applied to a camberline equation with an appropriate inertia function that defines the airfoil surface. For the present analysis the beam (wing) shape is known as a function of control deflections and it is desired to find the distributed moment that produces the commanded morphed shapes. Once the required moment is determined, it can be applied to the strain energy expression for normal stresses in a beam

$$U = \int_0^L \frac{M^2(x)}{2EI(x)} dx \tag{6}$$

This relationship determines the strain energy induced while creating a particular wing shape. Combining equations (5) and (6), the strain energy in terms of wing shape is

$$U = \frac{1}{2}\int_0^L \left(\frac{d^2\eta}{dx^2}\right)^2 EI(x)dx \tag{7}$$

A solid airfoil section with an arbitrary modulus of elasticity and span thickness will be used to define the inertia function in equation (7). Using the airfoil thickness expressions that accompany the NACA 4-series airfoils, the inertia function is defined as

$$I(x) = \frac{t}{4} y_t(x)^3 \cos^3\theta \tag{8}$$

where $\theta = \tan^{-1}(d\eta/dx)$, t is the section span thickness, and

$$y_t = t_c c\left(a_0\sqrt{x/c} - a_1(x/c) - a_2(x/c)^2 + a_3(x/c)^3 - a_4(x/c)^4\right) \tag{9}$$

In equation (9), t_c refers to the airfoil max thickness, and a_n are known shape coefficients.

Making the appropriate substitutions into equation (7) and carrying out the piecewise integration corresponding to the camberline function, the closed-form strain energy expression for a single wing section in a morphed state is

$$U = tEt_c{}^3c^2\left(f(H,P)\delta^2 + g(H,P)M\delta + h(H,P)M^2\right) \tag{10}$$

The functions *f*, *g* and *h* are highly nonlinear and primarily dependent on *H*. For a deviation in morphing states from an initial condition, the change in strain energy is

$$\Delta U = -tEt_c{}^3c^2\begin{pmatrix} f(H,P)\left(2(\delta 1)(\Delta\delta) + \Delta\delta^2\right) \quad + \\ g(H,P)\left((\Delta\delta)(M1) - (\Delta\delta)(\Delta M) - (\delta 1)\Delta M\right) \\ + \quad h(H,P)\left(2(M1)\Delta M + \Delta M^2\right) \end{pmatrix} \tag{11}$$

The function is negated so that a change to a larger displacement will result in negative work (work done by the actuators on the wing). It is the negative work that we ultimately want to minimize. The strain energy function is applied to each airfoil control actuator along the wingspan to define a total strain energy cost function for morphing the wing.

$$W_S = \sum_i^R \Delta U \tag{12}$$

Morphing Aerodynamic Energy

The goal of this section is to derive an expression for the aerodynamic work required to change the camber of a three-dimensional wing. This expression will be based on a standard vortex-lattice method[9]; therefore the validity of this analysis will be limited to that of a VLM (quasi-steady, potential flow, thin wing and small angles). The quasi-steady assumption limits this model to relatively slow control surface deflections.

Along with the camberline variables previously defined (*M*, *P*, *H*, and δ), additional nomenclature for this section is as follows:

- r = spanwise index (root to tip)
- n = chordwise index (leading edge to trailing edge)
- R = number of spanwise vortices on a half-span
- N = total number of chordwise vortices
- $a_{i,j}$ = influence of the mean camberline slope j on the vortex i
- $\psi_{i,j}$ = slope of the mean camber line ($d\eta/dx$) at the spanwise section i and chordwise section j
- U_{inf} = free-stream velocity
- τ = represents the time between the initial (τ=0) and final deflections (τ=1)
- $M1_i$ = magnitude of maximum at the spanwise location i at $\tau = 0$
- $\delta 1_t$ = trailing edge deflection at the spanwise location i at $\tau = 0$
- b = wing span
- η = z coordinates of the mean camber line
- $\bar{c}$ = mean geometric chord

From a standard VLM, the circulation on a wing can be represented as

$$\begin{aligned} \bar{\Gamma}_{Camber_k} &= \frac{\Gamma_{Camber_k}}{U_{\inf}} = \sum_{r=1}^{R}\sum_{n=1}^{N} a_{k,(r-1)N+n}\psi_{r,n} \\ \bar{\Gamma}_{\alpha_k} &= \frac{\Gamma_{\alpha_k}}{U_{\inf}} = -\sum_{r=1}^{R}\sum_{n=1}^{N} a_{k,(r-1)N+n} \\ \bar{\Gamma}_k &= \bar{\Gamma}_{\alpha_k}\alpha + \bar{\Gamma}_{Camber_k} \end{aligned} \tag{13}$$

The slope of the mean camber line ($\psi_{r,n}$) will be defined at each spanwise section as a function of independent camber values (M_r) and trailing edge deflections (δ_r). Defining $A_{r,n}$ and $B_{r,n}$, as constants that relate M_r and δ_r, the expression for $\psi_{r,n}$ is

$$\psi_{r,n} = \frac{d\eta}{dx} = A_{r,n}M_r(\tau) + B_{r,n}\delta_r(\tau) \tag{14}$$

It is seen in equation (14) that M_r and δ_r are functions of the non-dimensional time τ. This is done because the aerodynamic work must be calculated over a given time step, and defining τ allows the variation of M_r and δ_r during the time step to be defined. For simplicity, it will be assumed that M_r and δ_r vary linearly between their initial and final values, and therefore can be represented as

$$\begin{aligned} 0 \le \tau \le 1 \\ M_r = \Delta M_r\tau + M1_r \\ \delta_r = \Delta\delta_r\tau + \delta 1_r \end{aligned} \tag{15}$$

where $M1_r$ and $\delta 1_r$ represent the values at the beginning of the time step, and ΔM_r and $\Delta\delta_r$ represent the change that occurs during the time step. Combining equations (13) and (14) allows the circulation on the wing to be written explicitly for M_r and δ_r.

$$\overline{\Gamma}_k = \sum_{r=1}^{R}\left[C_{k,r}M_r + D_{k,r}\delta_r\right] + \sum_{r=1}^{R}E_{k,r}\alpha$$
$$C_{k,r} = \sum_{n=1}^{N} a_{k,(r-1)N+n}A_{r,n}$$
$$D_{k,r} = \sum_{n=1}^{N} a_{k,(r-1)N+n}B_{r,n} \quad (16)$$
$$E_{k,r} = -\sum_{n=1}^{N} a_{k,(r-1)N+n}$$

The generic work equation is

$$Work = \int_{r_1}^{r_2} F(r)\cdot dr \quad (17)$$

where the force F is integrated over the path of r. If r is a function of time, dr can be written as

$$dr(t) = \frac{dr}{dt}dt \quad (18)$$

In calculating the aerodynamic work, it is required to evaluate equation (17) on each panel of the wing. The dr/dt term in (18) is the change in the camberline at each panel, and can be represented as

$$\phi_{\bar{r},\bar{n}} = \frac{d\eta}{d\tau} = \left(T_{\bar{r},\bar{n}}\Delta M_{\bar{r}} + Q_{\bar{r},\bar{n}}\Delta\delta_{\bar{r}}\right)c_{\bar{r}} \quad (19)$$

These values are calculated at the chordwise location of the vortex on each panel. The force term in equation (17), obtained from the Kutta-Joukowski Theorem, is

$$F = \rho U_{\inf}\Gamma \quad (20)$$

Using equation (20), the lift on each panel can be written as

$$L_{(\bar{r}-1)N+\bar{n}} = \rho U_{\inf}\Gamma_{(\bar{r}-1)N+\bar{n}}\frac{b}{2R} \quad (21)$$

From equations (17-21), the aerodynamic work on each panel can be expressed as an integral between the initial and final τ values.

$$\frac{\overline{W}_{(\bar{r}-1)N+\bar{n}}}{\rho U_{\inf}{}^2 S\bar{c}} = \frac{b}{2SR\bar{c}}\int_0^1 \overline{\Gamma}_{(\bar{r}-1)N+\bar{n}}\phi_{\bar{r},\bar{n}}d\tau \quad (22)$$

The only term in equation (22) dependent upon τ is the circulation. From equations (15) and (16), this integral works out very simply to

$$\frac{\overline{W}_{(\bar{r}-1)N+\bar{n}}}{\rho U_{\inf}{}^2 S\bar{c}} = \frac{b}{2SR\bar{c}}\sum_{r=1}^{R}[(C_{(\bar{r}-1)N+\bar{n},r}(0.5\Delta M_r + M1_r)) + D_{(\bar{r}-1)N+\bar{n},r}(0.5\Delta\delta_r + \delta 1_r) + E_{(\bar{r}-1)N+\bar{n},r}\alpha]\left(T_{\bar{r},\bar{n}}\Delta M_{\bar{r}} + Q_{\bar{r},\bar{n}}\Delta\delta_{\bar{r}}\right)c_{\bar{r}} \quad (23)$$

It should be noted that equation (23) assumes the angle of attack remains constant. Also, the sign convention used here means that negative values require that work be put into the system. The aerodynamic work for the entire wing (both sides) is

$$\widetilde{W}_a = \frac{W_a}{\rho U_{\inf}{}^2 S\bar{c}} = 2\sum_{\bar{r}=1}^{R}\sum_{\bar{n}=1}^{N}\frac{\overline{W}_{(\bar{r}-1)N+\bar{n}}}{\rho U_{\inf}{}^2 S\bar{c}} \quad (24)$$

Following the above derivation, ΔC_L and ΔC_M may be represented as

$$\Delta C_{L_{Camber}} = \frac{2b}{SR}\sum_{k=1}^{RN}\Delta\overline{\Gamma}_{Camber_k}$$
$$C_{L_\alpha} = \frac{2b}{SR}\sum_{k=1}^{RN}\overline{\Gamma}_{\alpha_k} \quad (25)$$
$$\Delta C_L = C_{L_\alpha}\Delta\alpha + \Delta C_{L_{Camber}}$$

$$\Delta C_{M_{Camber}} = \frac{2b}{SRc_{MAC}}\sum_{k=1}^{RN}(x_{CG} - x_k)\Delta\overline{\Gamma}_{Camber_k}$$
$$C_{M_\alpha} = \frac{2b}{SRc_{MAC}}\sum_{k=1}^{RN}(x_{CG} - x_k)\overline{\Gamma}_{\alpha_k} \quad (26)$$
$$\Delta C_M = C_{M_\alpha}\Delta\alpha + \Delta C_{M_{Camber}}$$

Minimum Energy Flight Control

The previous two sections have developed equations for the structural and aerodynamic work required to produce a change in wing shape. The purpose of this shape change is to produce either a ΔC_L, a ΔC_M, or both. It is clear that a valid optimization problem would be to find the change in wing shape that requires the minimum work while achieving the desired ΔC_L or ΔC_M. Past research has investigated planform shapes that minimize the hinge moment of conventional control surfaces[10]. The problem to be solved here will assume a given and fixed P and H. This narrows the problem to finding the minimum energy spanwise distribution of ΔM_r and $\Delta\delta_r$. Using Lagrange Multipliers and equations (12, 24, 25 and 26), one obtains a set of linear equations solvable for the minimum energy ΔM_r and $\Delta\delta_r$ values.

Example Problem

To illustrate the above method of calculating and minimizing the aerodynamic and structural work required to achieve a desired ΔC_L and ΔC_M, a simple example will be presented. For this example, the previously defined airfoil shapes will be used assuming that only the magnitude of maximum camber (M_r) is a variable. Therefore it is assumed that there is no trailing edge control surface. The problem to be solved is then to find the minimum work distribution of maximum camber values required to obtain a ΔC_L of 0.1 away from an initially uncambered wing at zero angle of attack. The planform for this example is shown in Figure 2 (P=0.4, λ=0.5, Λ_{LE}=26.56°, b=6 *ft*, and c_r=2 *ft*, x_{cg}=1 *ft*, U_{inf}=500 *ft/s*). A small number of panels are used (R=3, N=2). Although they do not accurately model the wing, they allow for the matrices and vectors from the required equations to be illustrated.

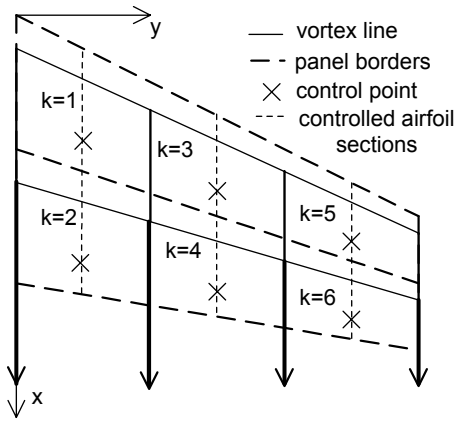

Figure 2. Panel Layout for the Example Problem

To begin, a standard vortex lattice method is applied to the planform to obtain the *a*-matrix required in equation (13). It is important to order the terms in *a* so that Γ_k and $\psi_{r,n}$ are consistent with the order of *k*-values shown in Figure 2.

$$a = \begin{bmatrix} -1.28 & -0.42 & -0.17 & -0.18 & -0.04 & -0.07 \\ 0.79 & -1.33 & -0.06 & -0.20 & -0.03 & -0.05 \\ -0.21 & -0.28 & -1.00 & -0.28 & -0.09 & -0.10 \\ -0.02 & -0.21 & 0.63 & -1.02 & -0.04 & -0.11 \\ -0.07 & -0.13 & -0.11 & -0.17 & -0.80 & -0.21 \\ -0.03 & -0.07 & -0.02 & -0.12 & 0.48 & -0.82 \end{bmatrix} \quad (27)$$

The equations for the slope of the mean camber line are obtained by differentiating equation (1) ($\bar{x}$ represents the *x* distance along the chord from the leading edge of each section and c_r is the size of the chord at each section).

$$\frac{d(\eta_r / c_r)}{d\bar{x}} = \frac{M_r}{P^2}\left[2P - 2\left(\frac{\bar{x}}{c_r}\right)\right] \quad 0 \le \frac{\bar{x}}{c_r} \le P \quad (28a)$$

$$\frac{d(\eta_r / c_r)}{d\bar{x}} = \frac{M_r}{(1-P)^2}\left[2P - 2\left(\frac{\bar{x}}{c_r}\right)\right] \quad P \le \frac{\bar{x}}{c_r} \le 1 \quad (28b)$$

The control points are located at $\bar{x}/c_r$ equal to 0.125 and 0.6125 on each spanwise section of the wing. It is seen in equation (14) that $\psi_{r,n}$ may be written in terms of $A_{r,n}$, M_r, $B_{r,n}$, and δ_r. For this example, only M_r is used to define the camber line, so $B_{r,n}$, and δ_r are set to zero. From equations (14, 28a and 28b), $A_{r,n}$ is

$$A_{r,n} = \begin{bmatrix} 0.313 & -2.64 \\ 0.313 & -2.64 \\ 0.313 & -2.64 \end{bmatrix} \quad (29)$$

Each row in (29) corresponds to a spanwise section, with the first row corresponding to the wing-root. The rows in (29) are identical because the same equation for the mean camber line was used for each section. From equation (15), M_r is represented as

$$M_r(\tau) = \begin{bmatrix} \Delta M_1 \tau \\ \Delta M_2 \tau \\ \Delta M_3 \tau \end{bmatrix} \quad (30)$$

In (30), the first row corresponds to the wing-root, and the last row to the wing-tip. The $C_{k,r}$ term in (16) can be calculated from (27) and (29). The $D_{k,r}$ and $E_{k,r}$ terms are not calculated because α is fixed at zero and δ_r is not being considered in this example.

$$C_{k,r} = \begin{bmatrix} -(1.28)0.313 + (0.42)2.64 & -(0.17)0.313 + (0.18)2.64 & -(0.04)0.313 + (0.07)2.64 \\ (0.79)0.313 + (1.33)2.64 & -(0.06)0.313 + (0.20)2.64 & -(0.03)0.313 + (0.05)2.64 \\ -(0.21)0.313 + (0.28)2.64 & -(1.00)0.313 + (0.28)2.64 & -(0.09)0.313 + (0.10)2.64 \\ -(0.02)0.313 + (0.21)2.64 & (0.63)0.313 + (1.02)2.64 & -(0.04)0.313 + (0.11)2.64 \\ -(0.07)0.313 + (0.13)2.64 & -(0.11)0.313 + (0.17)2.64 & -(0.80)0.313 + (0.21)2.64 \\ -(0.03)0.313 + (0.07)2.64 & -(0.02)0.313 + (0.12)2.64 & (0.48)0.313 + (0.82)2.64 \end{bmatrix} \quad (31)$$

The $\overline{\Gamma}$ equation in (16) can be written using the evaluated terms in (31) as

$$\begin{bmatrix} \Gamma_1 \\ \Gamma_2 \\ \Gamma_3 \\ \Gamma_4 \\ \Gamma_5 \\ \Gamma_6 \end{bmatrix} = \begin{bmatrix} 0.715 & 0.433 & 0.165 \\ 3.769 & 0.524 & 0.134 \\ 0.699 & 0.427 & 0.236 \\ 0.566 & 2.897 & 0.270 \\ 0.332 & 0.401 & 0.294 \\ 0.176 & 0.301 & 2.310 \end{bmatrix} \begin{bmatrix} \Delta M_1 \tau \\ \Delta M_2 \tau \\ \Delta M_3 \tau \end{bmatrix} \quad (32)$$

For this example α is being held zero, so in (25) and (26), $\Delta C_L = \Delta C_{L\ camber}$ and $\Delta C_M = \Delta C_{M\ camber}$.

$$\Delta C_L = \frac{(2)(6)}{(9)(3)}\left[6.25\Delta M_1 + 4.98\Delta M_2 + 3.41\Delta M_3\right]\tau \quad (33)$$

$$\Delta C_M = \frac{(2)(6)}{(9)(3)(1.56)}\left[-1.77\Delta M_1 - 2.40\Delta M_2 - 2.51\Delta M_3\right]\tau \quad (34)$$

Before the aerodynamic work at each panel is calculated from equation (22), it is first necessary to evaluate equation (19) at each panel. Equations (35a) and (35b) represent the distance moved at each panel between τ equal to zero and one. It is important to note that these terms are calculated at the chordwise location of the vortex at each panel, and not at the control point (as was the case with $\psi_{r,n}$).

$$0 \le \frac{\bar{x}}{c} \le P$$

$$\phi_{r,n} = \frac{d(\eta_r / c_r)}{d\tau} c_r = \frac{\Delta M_r}{P^2}\left[2P\left(\frac{\bar{x}}{c_r}\right) - \left(\frac{\bar{x}}{c_r}\right)^2\right] c_r \quad (35a)$$

$$P \le \frac{\bar{x}}{c_r} \le P$$

$$\phi_{r,n} = \frac{d(\eta_r / c_r)}{d\tau} c_r = \frac{\Delta M_r}{(1-P)^2}\left[1 - 2P + 2P\left(\frac{\bar{x}}{c_r}\right) - \left(\frac{\bar{x}}{c_r}\right)^2\right] c_r \quad (35b)$$

From equations (35a) and (35b), the $T_{r,n}$ values in equation (19) are evaluated to

$$T_{r,n} = \begin{bmatrix} 0.527 & 0.859 \\ 0.527 & 0.859 \\ 0.527 & 0.859 \end{bmatrix} \quad (36)$$

Equation (19) also requires the chord length at each section (c_r), which evaluates to the following

$$c_r = \begin{bmatrix} 1.83 \\ 1.50 \\ 1.17 \end{bmatrix} \quad (37)$$

Equations (32), (36) and (37) are combined with equation (22) to obtain the work (this expression will not be presented because of its size).

The strain energy function (11) was defined by selecting a hard rubber as the actuator material with a modulus of 1.24x10^5 *psi*. Each actuator section is a unit width and applying equation (11) results in the following strain energy expression

$$W_s(lb \cdot ft) = -(16.2\Delta M_1{}^2 + 10.8\Delta M_2{}^2 + 6.58\Delta M_3{}^2) \times 10^4 \quad (38)$$

Now, with expressions for the aerodynamic and structural work, the optimization procedure mentioned previously may be executed. To begin this procedure, a Lagrange expression is formed with constraints on ΔC_L and ΔC_M.

$$LE(\Delta M_1, \Delta M_2, \Delta M_3) = -\widetilde{W}_a - \widetilde{W}_s + \lambda_1(\Delta C_L - \Delta C_{L desired}) + \lambda_2(\Delta C_M - \Delta C_{M desired}) \quad (39)$$

The negative signs on the work terms are present because it is desired to minimize the negative work. From (39), the equations to be satisfied for minimum energy are

$$\frac{\partial LE}{\partial \Delta M_1} = \frac{\partial LE}{\partial \Delta M_2} = \frac{\partial LE}{\partial \Delta M_3} = 0$$
$$\frac{\partial LE}{\partial \lambda_1} = \frac{\partial LE}{\partial \lambda_2} = 0 \quad (40)$$

The solution to the equations in (40) for a $\Delta C_{L\ desired}$ of 0.1 and $\Delta C_{M\ desired}$ of zero are

$$\Delta M_1 = 0.052$$
$$\Delta M_2 = 0.015$$
$$\Delta M_3 = -0.051$$

where ΔM_1 corresponds to the root. For these deflections, the total non-dimensional work ($\widetilde{W}$) is -0.0768. If the ΔC_M constraint is not enforced, the resulting ΔM values are

$$\Delta M_1 = 0.014$$
$$\Delta M_2 = 0.016$$
$$\Delta M_3 = 0.018$$

In this case, $\widetilde{W}$ is -0.0095 and ΔC_M equals -0.04. The effect of removing the ΔC_M constraint is not surprising considering the difficulty in producing lift without producing pitching moment.

The above example assumed that the angle of attack remained constant between the initial and final states. If it is assumed that this is a flying wing, the minimum energy deflections can be found that account for angle of attack. If the aircraft is trimmed at the initial and final states, then ΔC_M equals zero, and from equation (26)

$$\Delta\alpha = -\frac{\Delta C_{Mcamber}}{C_{M_\alpha}} \quad (41)$$

If it is assumed that this change in α occurs slowly and linearly between the final and initial states, then the following term is substituted for α in equation (23)

$$-\frac{\sum_{k=1}^{RN}\sum_{r=1}^{R}\left\{\left[C_{k,r}\left(\frac{1}{2}\Delta M_r + M1_r\right) + D_{k,r}\left(\frac{1}{2}\Delta\delta_r + \delta 1_r\right)\right](x_{CG} - x_k)\right\}}{\sum_{k=1}^{RN}\sum_{r=1}^{R}(x_{CG} - x_k)E_{k,r}} \quad (42)$$

Applying this to the previous example and solving for the minimum energy ΔM's required for a ΔC_L of 0.1 results in

$$\Delta M_1 = -0.0013$$
$$\Delta M_2 = -0.0035$$
$$\Delta M_3 = -0.0066$$

The change in angle of attack produced by these deflections is 1.9°, and the $\widetilde{W}$ required is -5.73x10^{-4}. It is seen that the lift is produced entirely with angle of attack, and the ΔM's produce the pitching moment that allow the aircraft to change angle of attack. It should be mentioned that this is a stable flying wing, and the above results depend heavily on the static margin of the aircraft.

Morphing and Conventional Comparison

To compare the energy requirements of morphing and conventionally actuated aircraft, the above method is implemented numerically. The planform parameters for the test aircraft are shown in Table 1. The morphing aircraft has $\Delta\delta$ and ΔM capability on the outboard wing section as shown in Figure 3. There are five independent spanwise sections on the outboard section (R=5). The maximum camber (P) is located at 40% of the chord, and the trailing edge surface (H) begins at 60% of the chord. The conventional aircraft is equipped with an outboard and inboard flap as shown in Figure 4. The flaps are 20% of the chord. The conventional aircraft does not require structural work for flap deflections. The freestream velocity for this comparison is 600 *ft/s*.

The control energy required for the morphing and conventional aircraft to obtain a ΔC_L while allowing α

to change will be examined. This method is applied because it allows the aircraft to obtain the lift in the most natural way possible. As mentioned previously, this method assumes a slow and linear deflection process through the time-step.

Table 1. Vehicle Parameters

Span	30 *ft*
Sweep	34.9 °
Taper Ratio Distribution	0.308,0.461
Root Chord	18.14 *ft*

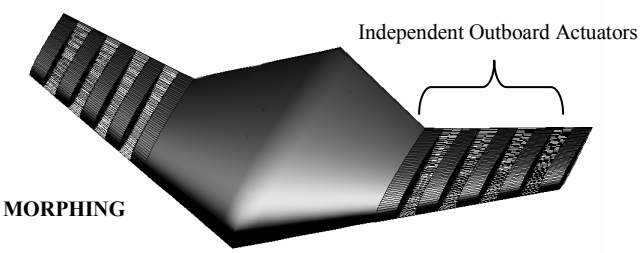

Figure 3. Morphing Aircraft Control Layout

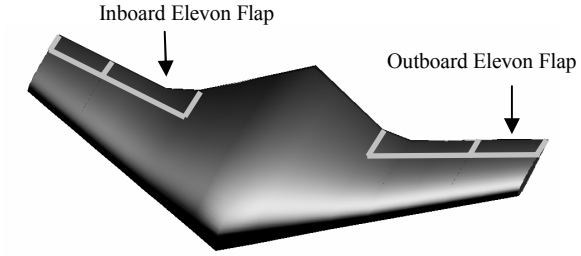

Figure 4. Conventional Aircraft Control Layout

Figure 5 shows the variation in the required aerodynamic work for the conventional and morphing aircraft. These are the resulting work values from the minimum energy deflections required to obtain a ΔC_L of 0.1 away from an initially uncambered aircraft. The positive values for the morphing aircraft indicate that the airstream produces forces in the direction of the required change in wing geometry. If there were no structural stiffness in the morphing aircraft, this would imply that no work would be required to obtain the change in lift.

A particularly interesting result seen in Figure 5 is the potential for the morphing aircraft to 'harvest' energy from the air-stream. Depending on the c.g. location of the vehicle, the airstream does aerodynamic work on the aircraft while generating a ΔC_L. In addition, from equation (23) we see that the aerodynamic work is a function of the squared velocity. As this velocity increases, the aerodynamic work approaches the structural work in overall weighting. Given appropriate internal actuators, a morphing vehicle might be flown that can gain energy from the airstream.

The modulus of elasticity used for the structure of the morphing aircraft was 1.24×10^5 *psi*, the common value used for hard rubber. The resulting structural work values for the morphing aircraft with various c.g. locations are shown in Figure 6. It is seen that, currently, the structural work far exceeds the aerodynamic work. As high compliance morphing designs become available, these values will decrease. It should be kept in mind that, for this analysis, an arbitrary structure is used with the primary purpose of holding the optimum morphing deflection values as small as possible. In addition, the strain energy acts as a restoring element for displacements back towards equilibrium.

Figures 5 and 6 show that as the aircraft approach neutral stability, the required work to change the lift becomes very small (accounting for the structural work in the morphing case). This is a result of the $C_{M\alpha}$ approaching zero, which from equation (41) implies that a small $\Delta C_{M\ Camber}$ value produces a very large change in angle of attack. Therefore, with the aircraft producing the majority of the ΔC_L with angle of attack, very little control deflections are necessary.

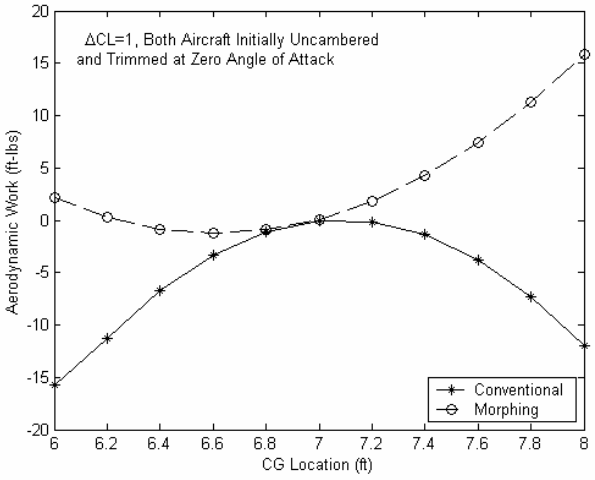

Figure 5. Effect of changing the CG location on the aerodynamic work required for a ΔC_L of 0.1

Figure 7 shows the spanwise distribution of trailing edge deflections, camber, and aerodynamic work required from the previous example with the c.g. at 7 *ft*. This is the optimum c.g. location for minimum aerodynamic work for the conventional aircraft, and near the worst c.g. location, in terms of required work, for the morphing aircraft. The inability of the morphing aircraft to obtain large positive (favorable) aerodynamic work is due simply to the fact that the deflections are held small by the overwhelming influence of the structural work. The large values of the structural work

overshadow the aerodynamic work in the optimization procedure.

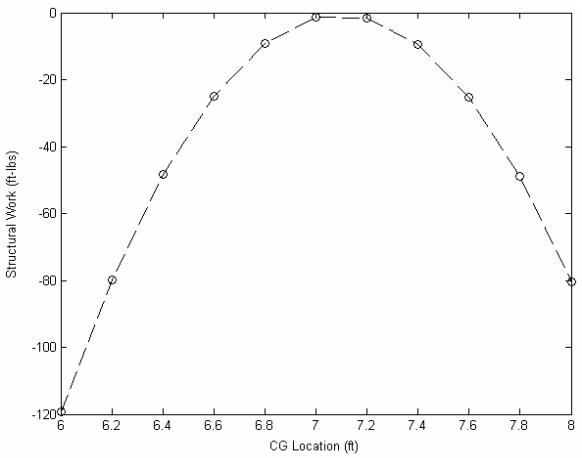

Figure 6. Effect of changing the CG location on the structural work required for a ΔC_L of 0.1

It is seen in Figure 7 that the morphing aircraft requires more trailing edge deflection than the conventional aircraft. This is counterintuitive to the notion that the structure in the morphing aircraft supposedly minimizes the deflections. This is a result of the chordwise distribution of the trailing edge deflection angle. For a conventional vehicle, the entire flap is deflected at the same commanded angle, whereas for the morphing deflection, only the trailing edge achieves the control angle. As seen in Figure 1, the entire trailing-edge control surface deflects in a distributed manner with the commanded angle realized only at the tip.

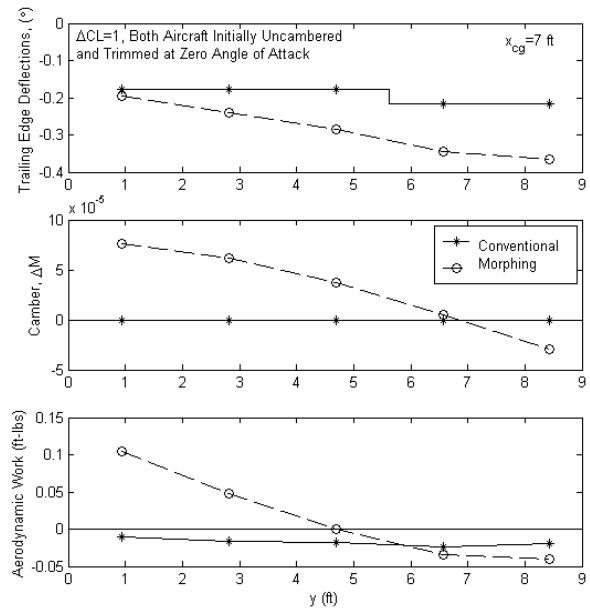

Figure 7. Spanwise distribution of the control deflections and aerodynamic work required for a ΔC_L of 0.1

Figure 8 shows the change in the spanwise distribution of minimum work $\Delta\delta$ and ΔM values when the modulus of elasticity is changed. It is seen that the trailing edge deflections near the tip decrease slightly with the increase in modulus and the camber values become slightly negative to account for this change. In general, the low modulus of elasticity permits greater control surface deflections. When the modulus of elasticity is low, the optimization algorithm attempts to minimize the negative aerodynamic work. That explains the work and deflection trends illustrated in Figure 8. The larger control surface deflections, camber in particular, induce greater (favorable) aerodynamic work.

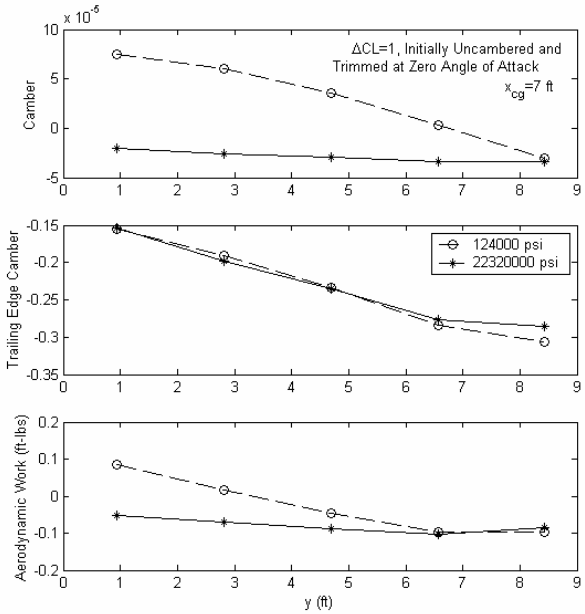

Figure 8. Spanwise distribution of the control deflections and aerodynamic work required for a ΔC_L of 0.1 at two different modulus of elasticity values

Conclusions

A complete, analytical model has been derived to predict the control energy requirements of morphing aircraft. The model required the development of unique aerodynamic and strain energy functions applied to adaptive wing shapes. Lagrange multiplier optimization was applied to minimize the energy functions under the constraint of achieving a particular change in lift coefficient. The final energy results were compared with a conventional vehicle in terms of variable c.g. location and optimized aerodynamic energy. Although morphing vehicles induce strain energy not produced by conventional aircraft, the independent spanwise deflection allow minimization of the aerodynamic energy requirements. At higher flight speeds and with advanced wing structures a morphing wing might supercede a conventional wing in flight control energy.

References

[1] Henderson, J.A., *et al.*, "Integrated Wing Design with Adaptive Control Surfaces," *42nd AIAA/ ASME/ASCE/AHS/ASC Structures, Structural Dynamics and Materials Conference*, Seattle, WA, April 16-19, 2001.

[2] Spillman, J., "The use of variable camber to reduce drag, weight and costs of transport aircraft," *Aeronautical Journal*, January 1992, v 96, pp1-8.

[3] Greff, E. "The development and design integration of a variable camber wing for long/medium range aircraft," *Aeronautical Journal*, November 1990, v 94, pp 301-312.

[4] Pettit, G., *et al*, "A Model to Evaluate the Aerodynamic Energy Requirements of Active Materials in Morphing Wings," Proceedings of DETC'01, 2001 ASME Design Engineering Technical Conferences, September 2001.

[5] Gern, F.H., Inman, D.J., and Kapania, R.K., "Computation of Actuation Power Requirements for Smart Wings with Morphing Airfoils," AIAA Paper 2002-1629, *43rd AIAA/ASME/ASCE/AHS/ ASC Structures, Structural Dynamics, and Materials Conference and Exhibit*, Denver, CO, April 22-25, 2002.

[6] Prock, B.C., Weisshaar, T.A., and Crossley, W.A., "Morphing Airfoil Shape Change Optimization with Minimum Actuator Energy as an Objective," AIAA Paper 2002-5401, *9th AIAA/ISSMO Symposium on Multidisciplinary Analysis and Optimization*, Atlanta, GA, September 4-6 2002.

[7] Mason, W.H., "Geometry for Aerodynamics," Department of Aerospace and Ocean Engineering, Virginia Tech, http://www.aoe.vt.edu/aoe/faculty/Mason_f/CAtxtTop.html

[8] Beer, F.P. and Johnston, Jr. E.R. *Mechanics of Materials, Second Edition*. McGraw-Hill: New York, 1992

[9] Katz, J., and Plotkin, A., *Low Speed Aerodynamic-Form Wing Theory to Panel Methods*, McGraw-Hill , 1991.

[10] Jones, R.T. and Cohen, D., "Determination Of Optimum Plan Forms For Control Surfaces", NACA TN No. 585, 1942.